THE JOURNAL OF NAVIGATION (2013), **66**, 17–33.
doi:10.1017/S037346331200032X

Performance Enhancement of Large-Ship Transfer Alignment: A Moving Horizon Approach

Dongfang Yang[1,2], Shicheng Wang[1], Hongbo Li[1,2], Zhiguo Liu[1] and Jinsheng Zhang[1]

[1] (*Xi'an High Tech Institution, China*)
[2] (*State Key Laboratory on Intelligent Technology and Systems, Tsinghua University, China*)
(E-mail: ydf09@mails.tsinghua.edu.cn)

In shipborne Transfer Alignment (TA) applications, partial observability is one of the most important factors limiting convergence velocity. This paper proposes a new method of attributing weak observable states and lever-arm variables to a group of constraints in order to improve the observability of TA model. This yields the so-called Constrained Transfer Alignment (CTA) model which is uniformly observable even under zero-manoeuvre conditions. Within this framework, the Moving Horizon Estimation (MHE) and its stability analysis are also addressed. Finally, comparative simulation results are given to demonstrate the advantages of the proposed approach.

KEY WORDS

1. Rapid Transfer Alignment (RTA). 2. Shipborne Inertial Systems. 3. Observability Analysis. 4. Moving Horizon Estimation (MHE).

Submitted: 29 March 2012. Accepted: 14 June 2012. First published online: 30 July 2012.

1. INTRODUCTION. Inertial Navigation System (INS) is a type of dead-reckoning navigation system and must to be initialized prior to its operation (Pitman, 1962). In many practical applications, the higher accuracy Master INS (MINS) is available to aid the alignment of the Slave INS (SINS). This process is appropriately known as Transfer Alignment (TA), and its significance has been recognized in both theoretical research and in modern navigation applications.

The past few decades have witnessed a marked rise in TA techniques to meet the increasing demands of quick reaction performance in weapons systems. Because weak observability is commonly considered the best starting point to lengthen the required time in the aligning process (Groves, 2003), most previous literatures endeavoured to increase the observability magnitude of the misaligned states. Bar-Itzhack proposed a framework of observability analysis of time-varying system in (Meskin and Itzhack,

1992a; 1992b). Within this framework, the manoeuvring-related observability during the in-flight alignment was investigated in (Itzhack and Porat, 1980), (Porat and Itzhack, 1981), and (Meskin and Itzhack, 1992). Rhee expanded the instantaneous observability results to the integrated INS/Global Positioning System (GPS) system in (Rhee et al., 2004). In the presence of time correlated noise, Wendel presented a rapid TA scheme (Wendel et al., 2004) where the full observability was achievable with brief Wing Rock (WR) manoeuvres. In order to excite azimuth-related states to extreme magnitude, Efraim proposed a new in-drilling alignment procedure (Efraim and Mintchev, 2007a; 2007b). Furthermore, TA experiments were designed in various practical platforms, such as F-16 fighters (Kevin and William, 1998) and other air-to-surface weapons (Ross and Elbert, 1994). More recently, diverse observability analysis results were summarized and the general analysis tools were given (Lee et al., 2010; Hong et al., 2008). Based on these literatures, since more latent states can be excited by vehicle motion, artificial manoeuvres are necessary to drive the alignment model to a uniformly observable one. However, as pointed out in Groves (2003), due to the existence of lever-arm, the manoeuvre motion can result in greater measurement uncertainty accompanied by increased flexure and vibration, which reduces the observability of INS error-states. In addition, challenges arise and the manoeuvres may be very difficult or even impossible to implement because of the huge inertia of warships in shipborne applications.

Motivated by the above observations, this paper presents a novel framework to achieve fast alignment performance with reduced-manoeuvre (or even zero-manoeuvre) demands. Under this framework, the traditional TA model is equally described as a definitely observable system subject to a group of state-constraints, which is the so-called Constrained Transfer Alignment (CTA) model. The corresponding constrained estimation problem can be solved by employing some newly presented filters as surveyed by Simon (2010).

The remainder of this paper is organized as follows. In Section 2, the traditional TA problem is formulated. Based on this, the CTA model is derived and analysed in Section 3, where the convergent performance of the Moving Horizon Estimator (MHE) in the CTA model is also proved. Finally, simulation results with different manoeuvres and concluding remarks are presented in Section 4 and Section 5, respectively.

2. PROBLEM FORMULATIONS.

2.1 *Glossary of Terms.*

n = Local navigation frame of axes
b = Real body frame of axes
b^* = Computed body frame of axes
C_a^b = Direction cosine transformation between a-frame and b-frame
$\mathbf{v}$ = Velocity, m/s
$\mathbf{a}$ = Acceleration, m/s^2
ψ = Attitude angle
∇ = Instrument error vector of accelerometers
ε = Instrument error vector of gyros
Δx = Variable displacement vector

2.2. *Formulations.* In Kain and Cloutier (1989), the framework of TA via velocity matching is presented by the following differential equations:

$$\Delta\dot{\mathbf{v}} = \Delta\psi \times C_{b^*}^{n}\mathbf{a}_{s}^{b} + C_{b^*}^{n}(\mathbf{a}_{fb}^{b} + \nabla_{a}^{b}), \tag{1}$$

$$\Delta\dot{\psi} = C_{b^*}^{n}(\omega_{fb}^{b} + \varepsilon_{g}^{b}), \tag{2}$$

where:

$\Delta\mathbf{v}$ is velocity difference between the master and slave velocities.
$\Delta\psi$ denotes the 'misalignment' of the slave INS b*-frame from the 'true' North-East-Down (n-frame).
$C_{b^*}^{n}$ is the estimated body-to-navigation frame direction cosine transformation.
$\mathbf{a}_{fb}^{b}$ denotes the flexible body acceleration which is equal described by a stochastic process.
∇_{a}^{b} and ε_{g}^{b} are parameterized instrument error vectors of accelerometer and gyros, respectively.
ω_{fb}^{b} is the flexible body rotation rate.

As pointed out (Britting, 1971; Itzhack and Porat, 1980; Yi, 1987 and Wendel et al., 2004), the accelerometer and gyro instrument error parameterization is very complex for accurate modelling. However, most literatures consider the random error of gyros as a mixture of three independent elements that will be referred to hereafter as successive start drifting ε_{bi}, random walk ε_{ri} and white noise signals w_g. Consequently, ε_{bi} and ε_{ri} can be formulated as:

$$\dot{\varepsilon}_{bi} = 0 \qquad i = x, y, z, \tag{3}$$

$$\dot{\varepsilon}_{ri} = \frac{-1}{\tau_g}\varepsilon_{ri} + w_{ri} \quad i = x, y, z, \tag{4}$$

where τ_g means the correlated time of gyros' output.

The total error of gyro is:

$$\varepsilon_g = \varepsilon_b + \varepsilon_r + w_g. \tag{5}$$

The instrument error of accelerometer ∇ is modelled as a mixture of random constant ∇_b and white noise w_a:

$$\nabla_i = \nabla_{bi} + w_{ai} \quad i = x, y, z, \tag{6}$$

where $\dot{\nabla}_{bi} = 0, i = x, y, z$.

Generally speaking, the commonly selected states include $\nabla\mathbf{v}$, $\nabla\Psi$, ε_{gi} and ∇_i, $i = x, y, z$. It is worth noting that some additional states can also be augmented into other TA models. However, for simplicity, those states are not involved in this paper.

Let $\tilde{\mathbf{r}}$ be the lever-arm vector denoting the relative distance between the SINS with respect to the MINS. Then the relationship between velocity of the MINS and the SINS can be shown (Sun and Deng, 2009), as:

$$\tilde{\mathbf{v}}_{s}^{n} = \mathbf{v}_{m}^{n} + \omega_{en}^{n} \times \tilde{\mathbf{r}}^{n} + \dot{\tilde{\mathbf{r}}}^{n} + \delta v, \tag{7}$$

where $\tilde{\mathbf{r}} = \mathbf{r} + \delta\mathbf{r}$.

The lever-arm compensation on the velocity output of the MINS can be calculated as follows:

$$\mathbf{v}_m^{comp} = \mathbf{v}_m^n + C_a^n[(\omega_{ia}^a - \omega_{ie}^a) \times \mathbf{r}^a]. \tag{8}$$

Then the measurement equation for velocity matching case in traditional TA takes the following form:

$$\mathbf{Z}_v = \tilde{\mathbf{v}}_s^n - \mathbf{v}_m^{comp} = \Delta\mathbf{v} + C_a^n(\omega_{ea}^a\times)\delta\mathbf{r}^a + \upsilon_v, \tag{9}$$

where:

$\upsilon_v = C_a^n \dot{\mathbf{r}}^a$ and can be seen as white measurement noise.
$\delta\mathbf{r}$ represents the lever-arm error vector and can be modelled as random constants.

Then, the traditional TA model consists of Equations (1)–(6) and Equation (9). Based on this traditional formulation, the objective of this paper is to obtain an equal TA framework with uniform observability.

3. MAIN RESULTS.

3.1 *Constrained Descriptions of Instrumental Errors and Lever-Arm.* Without loss of generality, the random walk component in Equation (4) is widely accepted as a first-order Gauss-Markov process. Suppose the inertial outputs are sampled with unit interval, the correspondingly discrete model can be written as:

$$\varepsilon_r(k+1) = \frac{\tau_g - 1}{\tau_g}\varepsilon_r(k) + w_r(k+1), \tag{10}$$

$$w_r(k+1) \sim \mathbf{N}(0, \sigma_r^2), \tag{11}$$

$$\varepsilon_b(k+1) = \varepsilon_b(k), \tag{12}$$

$$w_g(k+1) \sim \mathbf{N}(0, \sigma_w^2), \tag{13}$$

The correlated time of gyros τ_g is generally longer than several hundreds of seconds. Substituting Equations (10)–(13) into Equation (5) yields:

$$\varepsilon_g(k+1) = \varepsilon_r(k+1) + \varepsilon_b(k+1) + w_g(k+1) \sim \mathbf{N}(\varepsilon(k), (\sigma_r^2 + \sigma_w^2)). \tag{14}$$

Similarly, the accelerometer error in Equation (6) can be rewritten as:

$$\nabla(k) = \nabla_b + w_a(k) \sim \mathbf{N}(\nabla_b, \sigma_a^2). \tag{15}$$

It is worth noting that the above instrumental errors are represented in the slave body frame. Because the established instrumental error model varies with inertial instruments and modelling methods, for simplicity, we only consider a well-accepted instrumental error model here. However, it is easy to extend this constrained description framework to other error models.

On the other hand, the effects of lever-arm motion and ship flexure remarkably confine the alignment accuracy and rapidity in the presence of ship-dynamics, which are rather difficult to compensate due to their strong uncertainties (Titterton and Farnborough, 1990). In this section, we suggest that the lever-arm can also provide auxiliary information to evaluate the initial misalignment-states. As depicted in Figure 1, the coupled relationships of relative velocity and angular rotation between

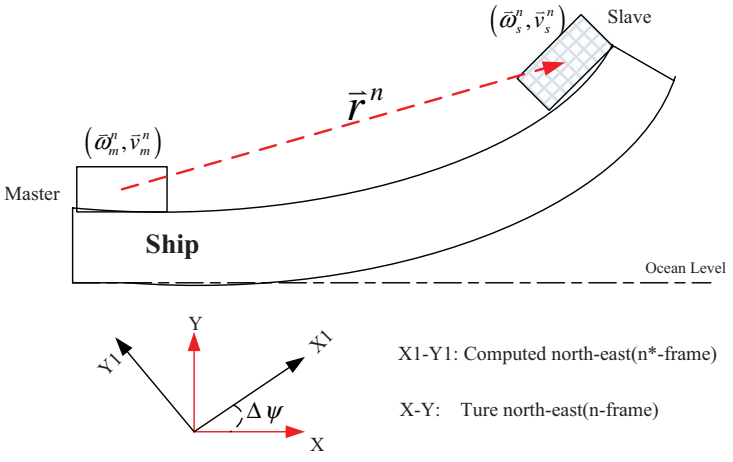

Figure 1. Coupled constraints description from lever-arm effect.

the MINS and SINS in the presence of dynamic deformation can be equally described as a group of constraints.

The relationship between relative linear velocity and angular velocity is well known as:

$$(\omega_s^n - \omega_m^n) \times \mathbf{r}^n = (\mathbf{v}_s^n - \mathbf{v}_m^n), \tag{16}$$

where ω_s^n can be arranged as:

$$\{[I + (\Delta\psi\times)]C_b^{n^*}(\tilde{\omega}_s^b) - \omega_m^n\} \times \mathbf{r}^n = \Delta\mathbf{v}. \tag{17}$$

Equations (14), (15) and (17) constitute the constrained descriptions of instrumental errors and lever-arm effect. The CTA model can be summarized as the following discrete-time form:

$$\mathbf{X}(k+1) = \mathbf{A}\mathbf{X}(k) + \mathbf{G}\mathbf{w}(k), \tag{18}$$

$$\mathbf{Z}(k) = \mathbf{H}\mathbf{X}(k) + v(k), \tag{19}$$

subject to:

$$\mathbf{w}(k) \sim \mathbf{N}\left(\begin{bmatrix} \varepsilon_g(k-1) \\ \nabla_b \end{bmatrix}, \begin{bmatrix} \sigma_r^2 + \sigma_w^2 & 0 \\ 0 & \sigma_a^2 \end{bmatrix}\right), \tag{20}$$

$$v(k) \sim \mathbf{N}(0, \sigma_m^2), \tag{21}$$

$$\Delta\mathbf{v} = \{[I + (\Delta\psi\times)]C_b^{n^*}(\tilde{\omega}_s^b) - \omega_m^n\} \times \mathbf{r}^n, \tag{22}$$

where:

$\mathbf{X} = [\Delta\psi_x, \Delta\psi_y, \Delta\psi_z, \Delta v_x, \Delta v_y, \Delta v_z]^T$ $(n-frame)$.
$\mathbf{G} = diag(C_{b^*}^n, C_{b^*}^n)$, σ_m^2 is the covariance of measurement noise.
$\mathbf{w} = [\varepsilon_{gx}, \varepsilon_{gy}, \varepsilon_{gz}, \nabla_x, \nabla_y, \nabla_z]$ $(b-frame)$ and $\mathbf{A}$ is derived by traditional TA model described in Equations (1) and (2).

3.2. *Observability Analysis on TA Models.* It is worth noting that the observability analysis of dynamic time-varying systems is still an open question. On the basis of observability analysing methods (Ham and Brown, 1983; Meskin and Itzhack, 1992a; 1992b), the observability analyses on traditional TA models were referenced in many previous literatures (e.g., Jiang and Lin, 1992; Fang and Wan, 1996). Generally speaking, the velocity and angular misalignment can be easily observed under proper measurement model, and it is hard to observe all the instrumental error uniformly at the same time. In this section, the observability analysis is introduced in the proposed CTA system.

Meskin and Itzhack (1992a; 1992b) have pointed out that the observability analysis of the time-varying alignment system at the jth segment, after having gone through segments 1, 2,..., j−1, has to be carried out on $\tilde{\mathbf{Q}}_j$, the Total Observability Matrix (TOM) at that segment. The matrix $\tilde{\mathbf{Q}}_j$ is constructed as follows:

$$\tilde{\mathbf{Q}}_j = \begin{bmatrix} \tilde{\mathbf{Q}}_1 \\ \tilde{\mathbf{Q}}_2 e^{\mathbf{A}_1\Delta_1} \\ \cdots \\ \tilde{\mathbf{Q}}_j e^{\mathbf{A}_{j-1}\Delta_{j-1}} \cdots e^{\mathbf{A}_1\Delta_1} \end{bmatrix}, \tag{23}$$

where:

$\tilde{\mathbf{Q}}_i^T = \left[\mathbf{H}_i^T | (\mathbf{H}_i\mathbf{A}_i)^T | (\mathbf{H}_i\mathbf{A}_i^2)^T | \ldots | (\mathbf{H}_i\mathbf{A}_i^{n-1})^T\right], 1 \leqslant i \leqslant j$, can be seen as the discriminant matrix of observability according to the classic control theory in the instantaneous case.

Δ_i is the time span of segment i.

Furthermore, the TA models constitute dynamic systems for which Theorem 2 in (Meskin and Itzhack, 1992a; 1992b) holds, thus we can use the Stripped Observability Matrix (SOM) $\tilde{\mathbf{Q}}_s(j)$ for simplicity. The SOM is constructed as:

$$\tilde{\mathbf{Q}}_s(j) = \begin{bmatrix} \tilde{\mathbf{Q}}_1 \\ \tilde{\mathbf{Q}}_2 \\ \cdots \\ \tilde{\mathbf{Q}}_j \end{bmatrix}. \tag{24}$$

For the constrained TA model in Equations (18)–(22), the instantaneous discriminant matrix in segment i is:

$$\tilde{\mathbf{Q}}_i^T = \left[\mathbf{H}_i^T | (\mathbf{H}_i\mathbf{A}_i)^T | (\mathbf{H}_i\mathbf{A}_i^2)^T | \ldots | (\mathbf{H}_i\mathbf{A}_i^5)^T\right] \tag{24a}$$

where:

$$H = \left[\mathbf{0}_{3\times3} \quad \mathbf{I}_{3\times3}\right]$$

$$A = \begin{bmatrix} A_{11} & A_{12} \\ A_{21} & A_{22} \end{bmatrix}, \quad A_{12} = \begin{bmatrix} 0 & \frac{-1}{R+h} & 0 \\ \frac{1}{R+h} & 0 & 0 \\ \frac{\tan L}{R+h} & 0 & 0 \end{bmatrix}, \quad A_{21} = \begin{bmatrix} 0 & -f_u & f_n \\ f_u & 0 & -f_e \\ -f_n & f_e & 0 \end{bmatrix}$$

$$A_{11}=\begin{bmatrix} 0 & \omega_{ie}\sin L+\frac{v_e\tan L}{R+h} & -\left(\omega_{ie}\cos L+\frac{v_e}{R+h}\right) \\ -\left(\omega_{ie}\sin L+\frac{v_e\tan L}{R+h}\right) & 0 & \frac{-v_n}{R+h} \\ \left(\omega_{ie}\cos L+\frac{v_e}{R+h}\right) & \frac{v_n}{R+h} & 0 \end{bmatrix}$$

$$A_{22}=\begin{bmatrix} \frac{v_n\tan L-v_u}{R+h} & 2\omega_{i}e\sin L+\frac{v_e\tan L}{R+h} & -\left(2\omega_{ie}\cos\lambda+\frac{v_e}{R+h}\right) \\ -2\left(\omega_{ie}\sin L+\frac{v_e\tan L}{R+h}\right) & \frac{-v_u}{R+h} & \frac{-v_n}{R+h} \\ 2\omega_{ie}\cos L+\frac{v_e}{R+h} & \frac{2v_n}{R+h} & 0 \end{bmatrix}$$

Please refer to (Britting, 1971) for details on the above notations. We can easily find that the rank of the SOM is uniformly equal to six even without any manoeuvring motion, which equally means that the constrained system is completely observable in every segment. See (Rao et al., 2003) for detailed definitions of observability.

3.3 *Moving Horizon Estimator and its Modified Version in CTA Case*. When it comes to the constrained estimation problem, various filters other than traditional Kalman filtering have been presented (Simon, 2010), such as projecting methods, unscented filtering and truncated particle filtering, etc. To maintain a trade-off between accuracy and calculating costs, the MHE (Muske and Rawlings, 1993), which stems from the Bayesian Maximum *a Posterior* (MAP), is modified to better suit the proposed framework. The Bayesian MAP estimation of x given y essentially means the most likely value of x, given y is:

$$\hat{x}_{map}=arg\max_{x} p(x\,|\,y) \tag{25}$$

Essentially speaking, MHE is an approximation of MAP estimation with a moving, fixed-size estimation window. The fixed-size estimation window is necessary to bound the size of the quadratic program. Most previous works assume that the noise among the system is mutually independent and the initial state and noise have (truncated) Gaussian distributions with zero means, where the posterior probability can be easily derived (Muske and Rawlings, 1993; Goodwin and Hernan, 2004), while in the CTA case as proposed in Equations (18) and (19), we take the varying means Gaussian distributions into account. That is:

$$\begin{aligned} p_{w(k)}(w) &\propto exp\left\{-\frac{1}{2}[w-w(k-1)]^T Q_k^{-1}[w-w(k-1)]\right\}, \\ p_{v(k)}(v) &\propto exp\left(-\frac{1}{2}v^T R_k^{-1}v\right), \\ p_{X(0)}(X) &\propto exp\left[-\frac{1}{2}\left(X-\overline{X_0}\right)^T P_0^{-1}\left(X-\overline{X_0}\right)\right], \end{aligned} \tag{25a}$$

where R, Q and P_0 are the covariance matrix of measurement noise, system noise and error covariance of initial states, respectively.

Using Bayes' rule, we have (Rao, 2000)

$$p(x_0, \ldots, x_T | y_0, \ldots, y_{T-1}) \propto p_{x_0}(x_0) \prod_{k=0}^{T-1} p_{v_k}(y_k - h_k(x_k)) p(x_{k+1}|x_k),$$
$$p(x_{k+1}|x_k) = p_{w_k}(x_{k+1} - f_k(x_k)). \tag{26}$$

Furthermore:

$$\begin{aligned} &arg \max_{\{x_0,\ldots,x_T\}} p(x_0, \ldots, x_T \,|\, y_0, \ldots, y_{T-1}) \\ &= arg \min_{\{x_0,\ldots,x_T\}} \sum_{k=0}^{T-1} ||v_k||^2_{R_k^{-1}} + ||w_k - w_{k-1}||^2_{Q_k^{-1}} + ||x_0 - \bar{x}_0||^2_{P_0^{-1}} \end{aligned} \tag{27}$$

where the minimization is done subject to the dynamics and all constraints. $|x||^2_Q = x^T Q x$, $w_{-1} = 0$ and the 'cost function' is defined as:

$$\Phi_T^* = \min_{x_0, \{w_k\}_{k=0}^{T-1}} \sum_{k=0}^{T-1} L_k(w_k, v_k) + \Gamma(x_0), \tag{28}$$

where:

$$\begin{aligned} &L_k(w_k, v_k) = \|v_k\|^2_{R_k^{-1}} + \|w_k - w_{k-1}\|^2_{Q_k^{-1}}, \\ &\Gamma(x_0) = \|x_0 - \bar{x}_0\|^2_{P_0^{-1}}. \end{aligned} \tag{28a}$$

Now we use a moving window (horizon) of length N, so the cost function can be rearranged as:

$$\Phi_T^* = \min_{x_0, \{w_k\}_{k=0}^{T-1}} \sum_{k=T-N}^{T-1} L_k(w_k, v_k) + \sum_{k=0}^{T-N-1} L_k(w_k, v_k) + \Gamma(x_0). \tag{29}$$

Define the arrival cost of a state $z \in R_{T-N}$ at time $T-N$ as:

$$Z_{T-N}(z) = \min_{x_0, \{w_k\}_{k=0}^{T-N-1}} \left\{ \sum_{k=0}^{T-N-1} L_k(w_k, v_k) + \Gamma(x_0) : x(T-N; x_0, 0, \{w_k\}) = z \right\}. \tag{30}$$

R_{T-N} denotes the reachable set of the state space subject to all constraints and dynamics of the system. Then the optimization problem of the proposed CTA model can be rearranged as:

$$\Phi_T^* = \min_{z \in R_{T-N}, \{w_k\}_{k=T-N}^{T-1}} \left[\sum_{k=T-N}^{T-1} L_k(w_k, v_k) + Z_{T-N}(z) \right], \tag{31}$$

subject to Equations (20)–(22), and the optimal solution of Equation (31) is the MHE.

3.4 *Stability Analysis of MHE in CTA Case.*

3.4.1 *Definition 1.* Definition 1 states "*A function* $f: R^n \to R^n$ *is a* ***K-function*** *if it is continuous, strictly monotone increasing,* $f(x) > 0$ *for* $x \neq 0$, $f(0) = 0$, *and* $\lim_{x \to \infty} f(x) = \infty$."

Suppose $f(.)$ is a K-function, then its inverse function f^{-1} is also a K-function. Actually, it is easy to prove that the space of K-functions is closed under addition, composition and positive scalar multiplication.

3.4.2. *Definition 2*. Definition 2 states "*An estimator is an asymptotically stable observer for the system*

$$x_{k+1} = f_k(x_k, 0) \quad y_k = h_k(x_k)$$

if, for every feasible initial condition x_0, *and for every* $\epsilon > 0$, *there correspondingly exists* $\delta > 0$ *and a positive integer* $\bar{T}$ *such that if* $|x_0 - \hat{x}_0|| \leqslant \delta$, *then* $|x(T; x_0, 0) - \hat{x}_T|| \leqslant \epsilon$ *for all* $T \geqslant \bar{T}$. *Furthermore, for all feasible* x_0, $\hat{x}_T \to x(T; x_0, 0)$ *as* $T \to \infty$."

3.4.3. *Theorem 1*. In the CTA case as described in Equations (18)–(22), for all $\hat{x}_0 \in \mathbb{X}_0$, the MHE is an asymptotically stable observer as defined in Definition 2.

3.4.4. *Proof*. The stability analysis procedure consists of the following three steps:

3.4.4.1. *Step 1*. The convergence of $\{\hat{\Phi}_k\}$: monotone non-decreasing and bounded above sequence is convergent.

Suppose the sequence $\{\hat{\Phi}_k\}$ is the moving horizon solution of Equation (29), we have:

$$\begin{aligned} \hat{\Phi}_T &= \min_{z \in R_{T-N}, \{w_k\}_{k=T-N}^{T-1}} \left[\sum_{k=T-N}^{T-1} L_k(w_k, v_k) + \hat{Z}_{T-N}(z) \right] \\ &= \sum_{k=T-N}^{T-1} L_k\left(\hat{w}_{k|T-1}^{mhe}, \hat{v}_{k|T-1}^{mhe} \right) + \hat{Z}_{T-N}(z). \end{aligned} \tag{32}$$

From the definition of arrival cost as described in Equation (30), we can easily find that:

$$\hat{\Phi}_T - \hat{\Phi}_{T-N} \geqslant 0. \tag{33}$$

Suppose $N \to \infty$, the global optimization of Equation (28) is determined as:

$$\Phi_T^* = \min_{x_0, \{w_k\}_{k=0}^{\infty}} \left\{ \sum_{k=0}^{\infty} L_k(w_k, v_k) + \Gamma(x_0) \right\}. \tag{34}$$

Because of the existence of the above infinite sum, the partial sum of Φ_T^* is limited by a certain bound, denoted as a constant C here, then:

$$\hat{\Phi}_T = \min_{x_0, \{w_k\}_{k=0}^{T-1}} \left\{ \sum_{k=0}^{T-1} L_k(w_k, v_k) + \Gamma(x_0) \right\} \leqslant C. \tag{35}$$

Thus we have proved the sequence $\{\hat{\Phi}_k\}$ is monotone non-decreasing and upper bounded. Hence, it is convergent, and the partial sum of $\{\hat{\Phi}_T\}$ tend to zero:

$$\sum_{k=T-N}^{T-1} L_k\left(\hat{w}_{k|\infty}^{mhe}, \hat{v}_{k|\infty}^{mhe} \right) \to 0 \quad T \to \infty \tag{36}$$

3.4.4.2. *Step 2*. $\forall$ K-function $\theta(.)$, $\forall \epsilon$, $\exists \zeta$ such that if $\|x\| \leqslant \zeta$, then $\theta(x) \leqslant \epsilon$. Thus for the convergence of sequence $\{\hat{\Phi}_k\}$, $\exists N_0$, if $T \geqslant N_0$, $\sum_{k=T-N}^{T-1} L_k(\hat{w}, \hat{v}) \leqslant \zeta$ hold, then $\forall \epsilon$, $\theta\left(\left\| \sum_{k=T-N}^{T-1} L_k(\hat{w}, \hat{v}) \right\| \right) \leqslant \epsilon$ is guaranteed.

3.4.4.3. *Step 3*. In this step we prove that there exists a positive integer $\overline{T}$ that for all $i > \overline{T}$, there correspondingly exists a K-function $\theta(.)$ that guarantees $|x_i - \hat{x}_i\| \leqslant \theta\left(\left\|\sum_{k=T-N}^{T-1} L_k(\hat{w}, \hat{v})\right\|\right)$.

Based on the aforementioned observability analysis, we can easily found that the CTA model is uniformly observable, which guarantees that there exists a positive integer N_1 and a K-function $\varphi(.)$ such that for any two states x_1 and x_2 (Rao et al., 2003):

$$\varphi(\|x_1 - x_2\|) \leqslant \sum_{j=0}^{N_1-1} \|y(k+j; x_1, k) - y(k+j; x_2, k)\|, \tag{37}$$

where: for all $k \geqslant 0$.

Specially, assume $k = 0$, then:

$$\varphi(\|x_0 - \hat{x}_0\|) \leqslant \sum_{j=0}^{N_1-1} \|y(j; x_0, 0) - y(j; \hat{x}_0, 0)\|. \tag{38}$$

According to the Cauchy-Schwarz inequality, the square form of Equation (39) can be rearranged as:

$$[\varphi(\|x_0 - \hat{x}_0\|)]^2 \leqslant N_1 \sum_{j=0}^{N_1-1} \|y(j; x_0, 0) - y(j; \hat{x}_0, 0)\|^2. \tag{39}$$

The relationship between system outputs according to different initial states can be arranged as:

$$\begin{aligned} y(j; x_0, 0) - y(j; \hat{x}_0, 0) = {} & HA^j(x_0 - \hat{x}_0) + HA^{j-1}G(w_0 - \hat{w}_0) + \ldots \\ & + HG(w_{j-1} - \hat{w}_{j-1}) + (v_j - \hat{v}_j). \end{aligned} \tag{40}$$

From the CTA model, we can easily establish that the group of functions $f_i(x) = k_i x$ ($k_i \in \{HA^j, HA^{j-1}G, \ldots, HG\}$) are all Lipschitz continuous functions. Correspondingly, there exists a group of constants $c_i \in \mathbf{R}^+ (i = 1, 2, \ldots, j+1)$, named as the Lipschitz constants of $f_i(.)$, such that:

$$|f_i(x_i - x_j)\| \leqslant c_i \|x_i - x_j\| \quad \forall x_i, x_j. \tag{41}$$

Using the Cauchy-Schwarz inequality repeatedly, Equation (40) can be rewritten as:

$$\begin{aligned} |y(j; x_0, 0) - y(j; \hat{x}_0, 0)|^2 \leqslant {} & (j+2)[c_1^2 \|(x_0 - \hat{x}_0)\|^2 + c_2^2 \|(w_0 - \hat{w}_0)\|^2 + \ldots \\ & + \|(v_j - \hat{v}_j)\|^2]. \end{aligned} \tag{42}$$

Suppose $\{(x_0 - \hat{x}_0), \hat{w}_0, \ldots, \hat{w}_{j-1}, \hat{v}_j\}$ are not simultaneously equal to zero, and the bounded-ness feature of the practical noise sequence $\{w_0, \ldots, w_{j-1}, v_j\}$ is taken into account, then we can infer that there exists $C_1 = max\{c_1^2, c_2^2, \ldots, c_{j+1}^2, 1\}$ and $C_2 \in \mathbf{R}$, such that:

$$|y(j; x_0, 0) - y(j; \hat{x}_0, 0)|^2 \leqslant (j+2) K_1 \left(\|x_0 - \hat{x}_0\|^2_{P_0^{-1}} + \sum_{k=0}^{j} L_k(\hat{w}, \hat{v}) \right). \tag{43}$$

Furthermore, the partial sum of the above inequality satisfies:

$$\sum_{j=0}^{N_1-1} \|y(j; x_0, 0) - y(j; \hat{x}_0, 0)\|^2 \leqslant K_2 \left[\|x_0 - \hat{x}_0\|^2_{P_0^{-1}} + \sum_{k=0}^{N_1-1} L_k(\hat{w}, \hat{v}) \right], \tag{44}$$

where $L_k(\hat{w}, \hat{v}) = \|\hat{w}_k - \hat{w}_{k-1}\|^2_{Q^{-1}} + \|\hat{v}_k\|^2_{R_0^{-1}}$.

Thus, from Equation (39), we have:

$$[\varphi(\|x_0 - \hat{x}_0\|)]^2 \leqslant K_3 \left[\|x_0 - \hat{x}_0\|^2_{P_0^{-1}} + \sum_{k=0}^{N_1-1} L_k(\hat{w}, \hat{v}) \right], \tag{45}$$

where $K_1 = C_1.C_2(Q+R+P_0)$, $K_2 = N_1(N_1+1)K_1$ and $K_3 = N_1K_2$.

By recalling the properties of K-function given before, we assume that there exists a function $\theta^{-1}(.)$, defined as $\theta^{-1}(||x_0 - \hat{x}_0||) = [\varphi(||x_0 - \hat{x}_0||)]^2 + r.||x_0 - \hat{x}_0||^2_{P_0^{-1}}$, $\forall r \in \mathbf{R}$, which also satisfies Definition 1. This equally means that there exists K-function $\theta(.)$ such that:

$$|x_0 - \hat{x}_0| \leqslant \theta\left(\sum_{k=0}^{N-1} L_k(\hat{w}, \hat{v}) \right). \tag{46}$$

Analogously, we can prove that Equation (47) still satisfies for $\forall i \geqslant 0$.

Retrospectively, from the conclusion achieved in Step 2, we can conclude that $\forall \epsilon > 0$, $\exists N_0$, if $i \geqslant N_0 - N$ holds, we have:

$$|x_i - \hat{x}_i| \leqslant \epsilon. \tag{47}$$

This completes the proof.

4. SIMULATIONS.

In this section, an illustrative example is given to demonstrate the effectiveness and applicability of the proposed methods.

The traditional TA model with velocity matching is formulated as Equations (1)–(9), and the proposed TA model is described in Equations (18)–(22). According to the performance index of commonly adopted inertial instruments, the simulation conditions are selected as:

$\varepsilon_{bi} = 1(deg/h)$.
$\nabla_b = 10\,\mu g$.
$Q = 10^{-10}\ diag\ (1, 1, 1, 100, 100, 100)$.
$R = 10^{-6}\ diag\ (1, 1, 1)$.
$\tau_g = 300\ (s)$.

The initial misalignments of SINS are assumed as:

$\Delta\psi = (10, 10, 10)^T\ (deg)$.
$\Delta\mathbf{v} = (1, 1, 1)^T\ (m/s)$.

It is worth noting that here we consider the constraints in Equation (29) as linear constraints according to the fact that if $x \sim \mathbf{N}(\bar{x}, \sigma^2)$ such that $p[-3\sigma \leqslant (x - \bar{x}) \leqslant 3\sigma] = 99{\cdot}7\%$. The length of moving window is selected as $N = 10$ and the manoeuvre schemes are designed according to the feasibility in warship cases.

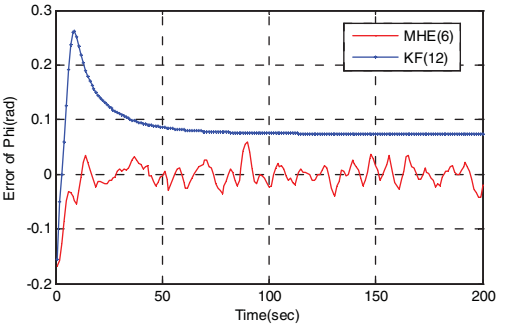

Figure 2. Estimation error of 'Phi'.

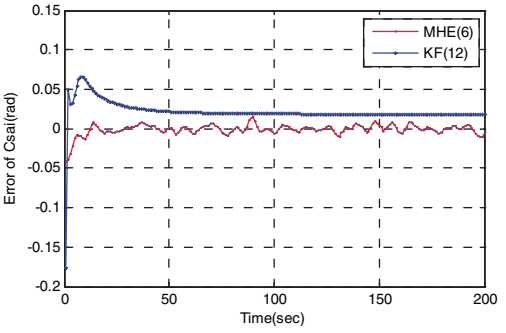

Figure 3. Estimation error of 'Csai'.

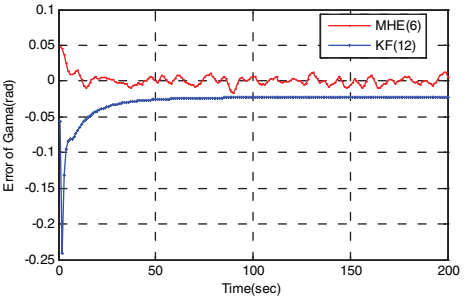

Figure 4. Estimation error of 'Gamma'.

4.1. *Scenario 1: Uniform Turn Motion*. In this scenario, the vehicle is assumed in uniform turn motion with approximate constant velocity and angular rotation. Here we suppose that the angular velocity in azimuth direction is $\omega_z = 1(°/s)$ and the linear velocity is $\mathbf{v} = (0{\cdot}5,\ 0{\cdot}5,0)^T(m/s)$. The simulation results of both traditional and CTA case are comparatively depicted in Figures 2–7.

4.2. *Scenario 2: 'Zero- Manoeuvre Motion'*. Here the vehicle manoeuvre is taken into consideration, and the consequent estimations of misaligned states are depicted in Figures 8–13.

As depicted in Figures 2–7, in traditional TA framework, if the uniform turn manoeuvre is available, the initial misalignment will converge to less than 0·05 rad

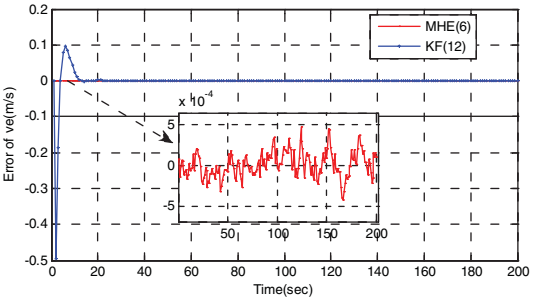

Figure 5. Estimation error of 've'.

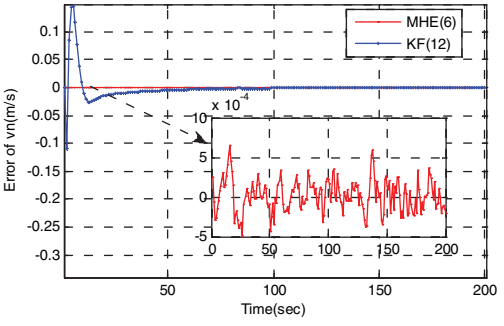

Figure 6. Estimation error of 'vn'.

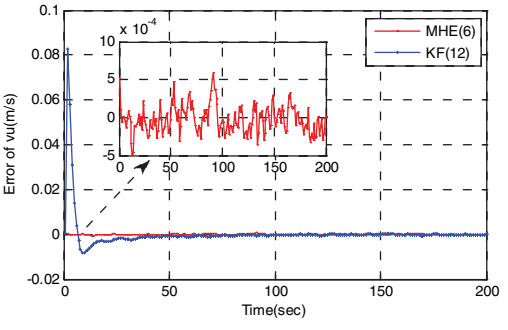

Figure 7. Estimation error of 'vu'.

and 0·001 (m/s) in nearly 50 seconds, respectively. While in the zero-manoeuvre motion case that as depicted in Figures 8–13, the estimation errors are nearly 0·1 rad and 0·001 (m/s) after 100 s. These results correspond with the fact that the weak observability of instrumental errors will indirectly decrease the evaluating accuracy of attitude and velocity states along with the coupled relationships among them (Rogers, 2002). Meanwhile, provided the proposed CTA framework is adopted, the initial misalignment on attitude and velocity states can approximately convergent to less than 0·01 rad and 0·001 (m/s) respectively in 10 s (the horizon window length of MHE).

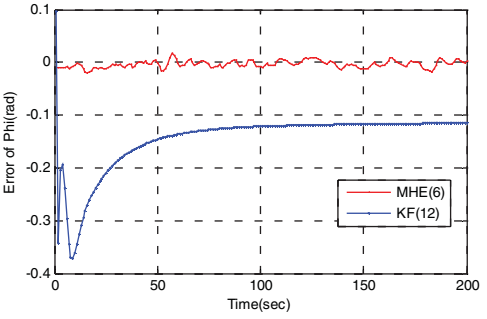

Figure 8. Estimation error of 'Phi'.

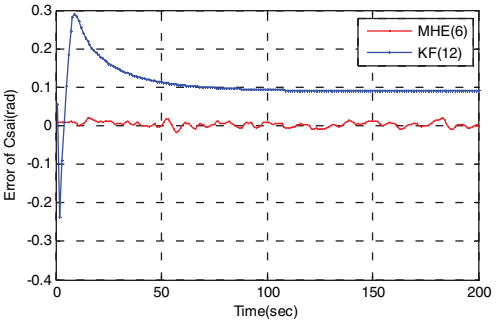

Figure 9. Estimation error of 'Csai'.

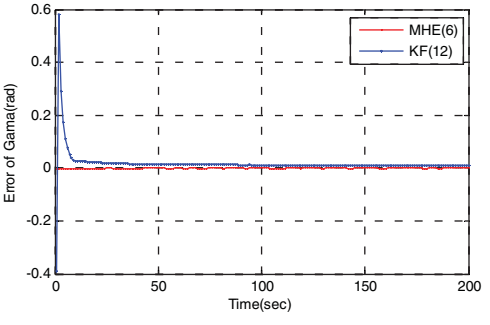

Figure 10. Estimation error of 'Gamma'.

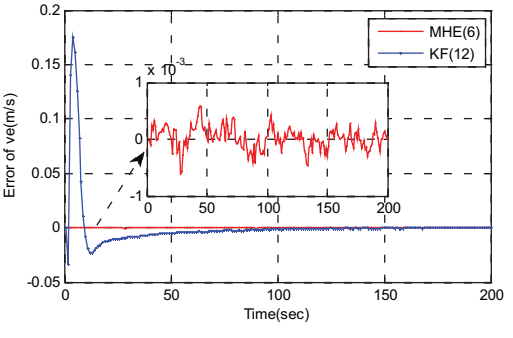

Figure 11. Estimation error of 've'.

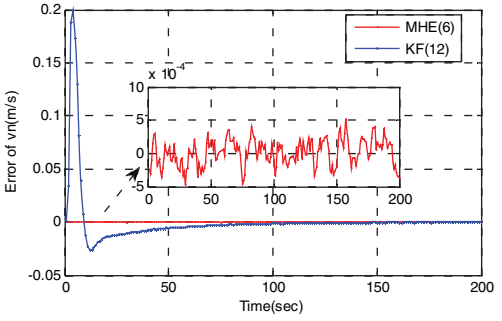

Figure 12. Estimation error of 'vn'.

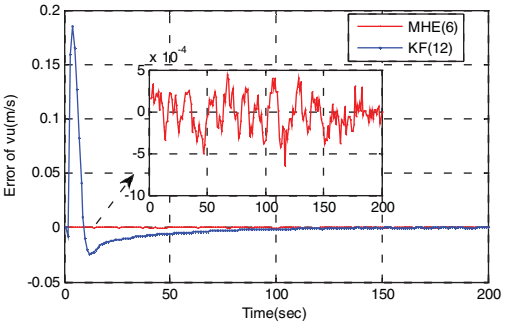

Figure 13. Estimation error of 'vu'.

5. CONCLUSIONS. In shipborne TA applications, the estimation of unobservable (or weak observable) states is the most time consuming process. In this paper, we consider a novel framework where all instrumental errors and the lever-arm vector are attributed to constraints, which yields rapid convergence of misalignment states. According to the observability analysis results, we can prove its uniform observability even in zero-manoeuvre circumstance. Subsequently, the MHE is adopted to solve the estimation problem and the corresponding stability analysis and simulations are also given to prove the effectiveness of the proposed TA framework.

Future work will focus on more practical cases with more cumbersome constraints and the calculation burden arising during the optimization process. However, along with the increasing power of computers, the framework of MHE-based state estimation will become an alternative for an expanding class of estimation applications, especially in weak observability applications.

ACKNOWLEDGEMENTS

The authors gratefully acknowledge the financial support of the National MOST and GAD through grant 2009CB724000, 2012CB821206 and 613121. The authors also express their thanks to the previous researchers and publishers, whose work inspired our intuition in this work.

REFERENCES

Britting, K. R. (1971). *Inertial Navigation System Analysis*. New York: Wiley.

Efraim, P. and Mintchev, M. P. (2007a). Observability Analysis for INS Alignment in Horizontal Drilling. *IEEE Transaction on Instrumentation and Measurement*. **56**(5), 1935–1945.

Efraim, P. and Mintchev, M. P. (2007b). Modeling of Observability During In-Drilling Alignment for Horizontal Directional Drilling. *IEEE Transaction on Instrumentation and Measurement*. **56**(5), 1946–1954.

Fang, J. C. and Wan, D. J. (1996). A Fast Initial Alignment Method For Strapdown Inertial Navigation System on Stationary Base. *IEEE Transaction on Aerospace and Electronic Systems*. **32**(4), 1501–1506.

Goodwin, G. C. and Hernan, H. (2004). A Moving Horizon Approach to Networked Control System Design. *IEEE Transcation on Automatic Control*. **49**(9), 1427–1445.

Groves, P. D. (2003). Optimising the Transfer Alignment of Weapon INS, *The Journal of Navigation*. **56**, 323–335.

Ham, F. M. and Brown, F. G. (1983). Observability, Eigenvalues and Kalman Filtering. *IEEE Transaction on Aerospace and Electronic Systems*. **19**(2), 269–274.

Hong, S., Chun, H. H., Kwon, S. H. and Lee, M. H. (2008). Observability Measures and their Application to GPS/INS. *IEEE Transaction on Vehicular Technology*. **57**(1), 97–106.

Itzhack, I. Y. and Porat, B. (1980). Azimuth Observability Enhancement During Inertial Navigation System In-Flight Alignment. *Guidance and Control*. **3**(4), 337–344.

Jiang, Y.E. and Lin, Y.P. (1992). Error Estimation of INS Ground Alignment Through Observability Analysis. *IEEE Transaction on Aerospace and Electronic Systems*. **28**(2), 92–97.

Kain, J. E. and Cloutier, J. R. (1989). Rapid Transfer Alignment for Tactical Weapon Applications. *Proceedings of AIAA Guidance, Navigation and Control Conference*, Boston, MA, US, 1290–1300.

Keerthi, S. S. and Gilbert, E.G. (1988). Optimal Infinite-Horizon Feedback Laws for a General Class of Constrained Discrete-Time Systems: Stability and Moving-Horizon Approximations. *Journal of Optimal Theory and Applications*. **57**, 265–293.

Kevin, J. S. and William, R. G. (1998). F-16 Flight Test for Rapid Transfer Alignment Procedure. *Proceedings of IEEE Position Location and Navigation Symposium*, Palm Springs, CA, 379–386.

Lee, M. H., Lee, J. H., Koh, Y. H., Park, H. G., Moon, J. H. and Hong, S. P. (2010). Observability and Estimability Analysis of the GPS and INS in the Vehicle. *Journal of Mechanical Systems for Transportation and Logistics*. **3**(3), 537–551.

Meskin, C. D. and Itzhack, I. Y. (1992a). Observability Analysis of Piece-Wise Constant Systems – Part I: Theory. *IEEE Transaction on Aerospace and Electronic Systems*. **28**(4), 1056–1067.

Meskin, D. G. and Itzhack, I. Y. (1992b). Observability Analysis of Piece-Wise Constant Systems - Part2: Application to Inertial Navigation In-Flight Alignment. *IEEE Transaction on Aerospace and Electronic systems*. **28**(4), 1068–1075.

Muske, K. R. and Rawlings, J. B. (1993). Receding Horizon Recursive State Estimation. *Proceedings of the American Control Conference*, San Francisco, California, 900–904.

Pitman, G. R. (1962). *Inertial Guidance*. New York: Wiley.

Porat, B. and Itzhack, I. Y. (1981). Effect of Acceleration Switching During INS In-Flight Alignment. *Journal of Guidance and Control*. **4**(4), 385–389.

Rao, C. V. (2000). *Moving Horizon Strategies for the Constrained Monitoring and Control of Nonlinear Discrete-Time Systems*. PhD thesis, University of Wisconsin-Madison.

Rao, C. V., Rawlings, J. B. and Mayne, D. Q. (2003). Constrained State Estimation For Nonlinear Discrete-Time Systems: Stability and Moving Horizon Approximations. *IEEE Transaction on Automatic Control*. **48**(2), 246–258.

Rhee, I., Abdel, M. F. and Speyer, J. L. (2004). Observability of an Integrated GPS/INS During Maneuvers. *IEEE Transaction on Aerospace and Electronic systems*. **40**(2), 526–535.

Rogers, R. M. (2002). Correlation and Convergence of Inertial Navigation System Error Models. *Proceedings of AIAA Guidance, Navigation and Control Conference and Exhibition*, Monterey California. AIAA 2002-4946, 1–11.

Ross, C. C. and Elbert, T. F. (1994). A Transfer Alignment Algorithm Study Based on Actual Flight Test Data from a Tactical Air-To-Ground Weapon Launch. *Proceedings of IEEE Position Location and Navigation Symposium*, 431–438.

Simon, D. (2010). Kalman Filtering with State Constraints: a Survey Of Linear And Nonlinear Algorithms. *IET Control Theory and Applications*. **4**(8), 1303–1318.

Sun, C. Y. and Deng, Z. L. (2009). Transfer Alignment of Shipborne Inertial-Guided Weapon Systems. *Journal of Systems Engineering and Electronics*. **20**(2), 348–353.

Titterton, D. H. and Farnborough, R. E. (1990). The Alignment of Ship Launched Missile Inertial Navigation Systems. *Proceedings of IEEE Inertial Navigation Sensor Development Colloquium*, London, 1–116.

Wendel, J., Jurgen, M. and Gert, F. T. (2004). Rapid Transfer Alignment in the Presence of Time Correlated Measurement and System Noise. *Proceedings of AIAA Guidance, Navigation and Control Conference and Exhibition*, Providence, Rhode Island, 1–12.

Yi, G. Q. (1987). *Principles of Inertial Navigation*. Beijing. Aviation Industry Press.